Journal of Engineering Research and Reports

Volume 26, Issue 5, Page 188-201, 2024; Article no.JERR.112128
ISSN: 2582-2926

Synthesis and Characterization of Crab Shell Based Magnetic Nanoparticles for the Remediation of Abattoir Waste Waters

Okpalaeze, Onyeka Anthony [a*] and Nkwocha, Promise Chibuzo [b]

[a] Nnamdi Azikiwe University, Nigeria.
[b] University of Uyo, Nigeria.

Authors' contributions

This work was carried out in collaboration between both authors. Both authors read and approved the final manuscript.

Article Information

DOI: 10.9734/JERR/2024/v26i51146

Open Peer Review History:
This journal follows the Advanced Open Peer Review policy. Identity of the Reviewers, Editor(s) and additional Reviewers, peer review comments, different versions of the manuscript, comments of the editors, etc are available here: https://www.sdiarticle5.com/review-history/112128

Original Research Article

Received: 04/01/2024
Accepted: 08/03/2024
Published: 19/04/2024

ABSTRACT

Meat and beef consumption rate in Nigeria has recorded increment leading to increase in abattoirs and lack of control in discarding the waste of the slaughtered animals has heightened the rate of ground water, air and environmental pollutions. In this paper, crab shell based magnetic Nanoparticles were utilized in the purification of waste water from abattoir. The factors considered in the purification process were pH, dosage, initial concentration, temperature and time and the response includes: bio-chemical oxygen demand (BOD), chemical oxygen demand (COD), turbidity and colour. Prior to the experimentation in the laboratory, the central composite design (CCD) of the experimental design was carried to determine the number of levels and the possible number of experimental runs during laboratory experiment. The outcome of the laboratory was used for the response surface methodology (RSM) of which linear and interaction model ware utilized in the

**Corresponding author: Email: oa.okpalaeze@unizik.edu.ng;*

determination of the relation between the factors and the responses and the model type was multiple input single output model system (all the factors equated to one response per time). Analysis of variance (ANOVA) tables was utilized in the determination of the model performance for each response to determine the best model suitable for the prediction of the responses. From the results obtained, the R-square values from the ANOVA table showed that the interaction model had a better prediction accuracy of 65.75%, 33.65%, 60.73% and 59.74% for the prediction of BOD, COD, turbidity and colour responses, respectively. The interaction model being the best was deployed for the generation of surface and contour plots to graphically obtain the optimal responses and factors that was utilized as a first guess to the optimization of the model and the final optimal response values obtained were 4.33mg/l, 128.9mg/l, 39.87% and 33.41% for BOD, COD, turbidity and colour, respectively at the optimal factor conditions of 5.5, 0.68g, 260mg/l, 335k and 50min for pH, dosage, initial concentration, temperature and time, respectively.

Keywords: Waste water treatment; abattoir; nanoparticles; responses; factors; modeling and optimization.

1. INTRODUCTION

Nanoparticle was defined in [1,2] as the characteristics of solid distribution having a size range of 10-1000nm. Most of the nanoparticles utilized are designed from many materials and components and such nanoparticles are known as nano-composites. Nanoparticles are usually synthesized from different sources mainly from natural and synthetic sources [3,4]. In this regard, the use of crab shell has been known to exhibit highly efficient characteristics for utilization in the waste water purification processes which its properties are due to biosorbent of its shell as the result of its high mechanical strength, strong structure and its capacity of withstanding extreme conditions during the nanoparticles synthesis process [3,5]. The papers from [4,6,7] made contributions in improving the waste water purification properties of the waste water which includes infusion of iron oxide into the internal structure with the aim of upgrading the magnetic properties of the nano-particle.

There are policies on waste water management and pollution in Nigeria but the inability to enforce the policies has been major cause of lack of disposal control as the abattoir waste are disposed to the environment and to the water bodies resulting to the death of aquatic animals. Some of the animal processes are performed close to a river causing nuisance to the aquatic bodies [8]. The waste water from abattoirs comprises of effluents from the slaughter house and with high amount of suspended solids, liquids and fats from the animals [9]. In Nigeria, there has been a high demand for meat, leading to the drive to maximize the meat production which has led to failure in adhering the good manufacturing practices during the meat processing and resulting to a total neglect of good hygiene practice and safety process [9,10]. The processing of meats from cows and other mammals requires large amount of water leading to the generation of large amount of suspended solids which affects both the surface water and the underground water because the processing of slaughtered animals generates urine, fats, blood and manure that are washed with water and sent to river bodies [11]. Hence, this paper presents the use of chito-protein nanoparticles obtained from crushed exoskeleton of crab shell for the purification of the waste water from slaughter houses. Characterization was carried out on the raw shell of the crab to determine the physicochemical properties. The nanoparticles prepared was used in the adsorption process of the waste water to determine the quantity of the responses. As guide to the laboratory experiment, CCD of experimental design was done with design expert to determine the amount of responses removed from the waste water. The responses were COD, BOD, turbidity and colour. The factors considered were pH, dosage, initial concentration, temperature and time. Linear and interactive RSM models were utilized in the development of relationship between the factors and the responses and ANOVA table was deployed for the determination of the performance of the models deployed to obtain the best model based on the prediction performance and genetic algorithm (GA) was utilized for the determination of the optimal responses and factors. The modeling was carried out in MatLab 2015a. The outcome of this paper would suggest means of purifying waste water from slaughter house was crab shell nanoparticles as the adsorbent.

2. LITERATURE REVIEW

In [12], coagulation/flocculation process was used at laboratory bench scale for the removal of chemical oxygen demand (COD), total suspended solids (TSS) and total phosphorus (TP) in abattoir wastewater. The wastewater was allowed to settle for 24 h and TSS and TP removal efficiencies of 65% and 32% were achieved, respectively. They used alum, ferric chloride and ferric sulfate during the coagulation/flocculation process. From their results, they observed that alum proved more effective in the reduction of TSS and TP present in the wastewater, whereas ferric sulfate was more effective in the reduction of COD. Increasing the dose of alum to 750 mg/l caused the removal efficiency of TP to reach 45%. According to the authors, the rate of removal of TP linearly increased with increasing doses of alum, resulting in a 98% removal efficiency of TP at 1000 mg/l dose of alum. At a 95% confidence interval, alum dose, coagulation velocity gradient/rapid mixing time (coagulation Gt) and flocculation velocity gradient/slow mixing time (flocculation Gt) were not significant for TSS removal efficiency, but alum dose was significant for TP removal. They also observed that the addition of a polyelectrolyte to an inorganic coagulant proved effective in the reduction of COD, TSS and TP, cut the amount of coagulant used and reduced the cost of the coagulation/flocculation process. A significant degree of particle elimination by size was produced by using alum; this improved further with the addition the polyelectrolyte.

In [13,14], the authors studied the slaughterhouse waste water treatment using combined chemical coagulation and electrocoagulation process. The authors employed the use of poly aluminium chloride (PACl) and applied voltage to the treatment of slaughter house waste water. An efficiency of more than 99% removal in the levels of BOD5 and COD was achieved by using a coagulant dose of 100mg/L and an applied voltage of 40V. Chemical coagulation of slaughterhouse wastewater has also been studied by adding aluminum salts and polymer compounds, and a maximum COD removal efficiency of 45–75% has been reported according to [15,16]. Polyaluminum chloride (PACl) was used as the flocculant to coagulate small particles into larger flocs that can be efficiently removed in the subsequent separation process of sedimentation and/or filtration. [17], studied the treatment of slaughterhouse wastewater characterized as having exceptionally high BOD, COD and TSS contents. The authors used a combined treatment system of coagulation and adsorption onto activated carbon, using different coagulants, such as alum, lime, ferrous sulfate, and ferric chloride used individually and in combination. A jar test method was applied to determine the optimal dose of these coagulants. From the results, they observed that increasing dosages of coagulants increased the sludge formation and COD removal. They observed that the volume of sludge was found to be an indicator of maximum removal of COD. From their studies, alum coagulant proved to be the best in removing COD up to 92%. Maximum sludge volume (400 ml/L) was also observed with alum. More than 90% removal efficiency in pollution load was observed at the set optimal conditions with coagulation process. A combination of coagulation and adsorption processes made negligible improvement in the removal efficiency of the system (as compared to the single process of coagulation) and removed pollution load up to 96%.

The author in [18] discovered that with inorganic flocculants, the effective species can be a solvated metal ion, which affect flocculation through double-layer compression and Schulze-Hardy effects and with an increase in pH, these species become charged and the mechanism of action changes. When the colloids are hydrophilic, e.g. humic acids, pH affects protonation. In presence of ionizable acidic or basic groups, colloid surface charge is affected by pH changes. In organic polymer flocculation as well, pH can affect polymer activity and the mechanism. From the research carried out in [19,20], it shows that pH of water adjusted with sulfuric acid and alum ranging from 5.0-8.0 gave an optimum pH of 7.0, and this gave the best color removal at about 76% and the turbidity removal around 80%. Research in [21] shows that the optimum value of pH depends essentially on the properties of the water treated, type of the coagulant used and its concentration. The results he obtained showed that the optimum initial pH for turbidity removal is 7 and 8.6 giving removal efficiencies of 95.9% and 95.2%, respectively. In research conducted in [22], higher concentration of effluent gives rise to decreased degree of flocculation, and the particles may be completely covered by the absorbed polymer layer. Higher concentration of effluent means higher amount of suspended particles and larger quantity of biodegradable materials contained in the water.

3. METHODS

3.1 Collection of Samples and Pre-processing

The waste water utilized in this study was obtained from the local abattoir located in Amansea in Awka south Local government area (LGA) Anambra State in south eastern Nigeria. The waste water sample was sieved to remove large suspended solids and other solids waste and the filtered sample was stored in a refrigerator. The crabshell was acquired from Onitsha Main market the Anambra state; the shells were washed, sundried and crushed to particle size of 75 microns.

3.2 Characterization of Waste Water Sample

The method utilized for the determination of COD in the waste water was from [23]. 10 ml of 0.25 N of potassium dichromate (k2Cr2O7) and 30 ml of sulphuric acid + silver nitrate reagent was prepared in 20 ml dilute sample. The mixture was re-fluxed for 2 hours and allowed to cool to a temperature of 28C. Distilled water will be used to dilute the solution making a volume of 150 ml. The remaining amount of potassium dichromate was titrated with ferrous ammonium sulphate (FAS) using ferrion indicator, the COD for each solution was obtained based on equation 1 below [23].

$$COD = \frac{(F_b - F_s) \times n \times 1000 \times 8}{V_s} \quad (1)$$

Where F_b represents amount of FAS in blank (ml), F_s represents the amount of FAS in the sample (ml), n represents the normality of FAS, the value 8 was taken as the equivalent weight of oxygen [24] and V_s represents the volume of the sample.

Turbidity meter and pH meter were used to determine the turbidity and pH of the waste water.

UV visible spectrophotometer was utilized at wavelength of 420nm to determine the colour of the sample.

3.3 Magnetic Composite Synthesis

Synthesis of the crabshell based magnetic nanoparticle was done in two stages as detailed in [20,22, 23,24]. Chito-protein was extracted from waste crabshell through de-protenization procedure with the utilization of sodium hydroxide. 500 ml of 2M NaOH solution was contacted with 100 g of crab shell using a magnetic hotplate stirring at 200 rpm and 65^{o}C for 2 hr. After cooling, the mixture was allowed to settle and then filtered. The filtrate was subjected to centrifugation and a clear liquid product was decanted to give way for highly concentrated radical protein sludge. The sludge product was dried at 1500 ^{o}C for 6 hr. The obtained chito-protein product was stored in a dry container for further utilization.

Ferromagnetite was synthesized via co-precipitation method with a molar ratio of 1:2 for Fe (II):Fe (III), respectively. The mixture was dissolved in de-ionized water and stirred at 50 rpm for 3 hr [4,7]. Subsequently, dried crabshell chito-protein was added to the solution in a ratio of 1:1. The mixture will be homogenized for 1 hr, followed by decantation. The formed precipitate was dried in an oven at 80 ^{o}C for 80 min. The resulting product will be labeled “MCSNC” which stands for magnetic crabshell nanocomposites, which will be used to facilitate the remediation of abattoir wastewater.

3.4 Design of Experiment

Based on literature survey, the table for range of values of the factors for abattoir waste water treatment with MCSNC was shown in Table 1.

The range values of the factors were entered in the design software application to generate the factor levels and shown in Table 2.

Table 1. Range of values for the factors

Factors	Range
pH	4-8
Dosage(g)	0.5-1.1
Initial concentration(mg/L)	100.5-400.5
Temperature (K)	310-345
Time (min)	15-50

Table 2. Factor levels

Factors	-alpha	-1	0	1	alpha
pH	3	4	6	8	9
Dosage(g)	0.35	0.5	0.8	1.1	1.25
Initial concentration(mg/L)	25.5	100.5	250.5	400.5	475.5
Temperature (K)	301.25	310	327.5	345	353.75
Time (min)	6.25	15	32.5	50	58.75

The outcome from the factor levels was used to generate the experimental runs that were taken to the laboratory for the purification of the waste water.

3.5 Laboratory Experiment for the Waste Water Purification

Five different concentrations of effluent were prepared prior to each batch adsorptive-coagulation experiment and the initial conditions of temperature, turbidity and absorbance were recorded. The pH of the samples was adjusted to desirable values using very few drops of 0.5 M sulphuric acid and (or) 0.5 M sodium hydroxide solutions. Different amounts of MCSNC were added and the five beakers was stirred simultaneously at 250 rpm for 3 min to initiate the coagulation process while the flocculation process was carried out by slow stirring at 20 rpm for 30 minutes, as described in [25,26]. After the slow stirring, the mixtures were allowed to settle by gravity, samples were withdrawn from the beaker and tested for the turbidity and color removal at different withdrawal time.

3.6 RSM Modeling and Optimization

To determine the best parameters for optimum colour and turbidity removal, Genetic algorithm (GA) optimization techniques will be adopted. Genetic algorithm (GA) entails a statistical exploration technique, capable of simulating a natural biological evolution is usually implemented in solving the optimization problems. The developed RSM model will be coupled with GA and used as a decision parameter in GA optimization (which occurs through a 4-staged cycle). The best sequence produced at the convergence of the loop becomes the solution to the optimization problem [27,28] GA optimization will be carried using the optimization toolbox of MATLAB R 2015 b (Matworks Inc.). The RSM models utilized were linear model and interaction models as shown in equations 2 and 3 respectively.

$$Y = a_o + a_1x_1 + a_2x_2 + a_3x_3 + a_4x_4 + a_5x_5 \quad (2)$$

$$Y = a_o + a_1x_1 + a_2x_2 + a_3x_3 + a_4x_4 + a_5x_5 + a_6x_1x_2 + a_7x_1x_3 + a_8x_1x_4 + a_9x_1x_5 + a_{10}x_2x_3 + a_{11}x_2x_4 + a_{12}x_2x_5 + a_{13}x_3x_4 + a_{14}x_3x_5 + a_{15}x_4x_5 \quad (3)$$

Where Y represents the responses (color, turbidity, COD and BOD) which implies that there was four models for each RSM models which represents each of the responses, x_1 to x_5 are the factors namely: pH, dosage, initial concentration, temp and time respectively.

4. RESULTS

4.1 Characterization

The waste water physicochemical characterization outcome was shown in Table 3.

The FTIR of the nanoparticle was shown in Fig. 1.

The crab shells gave a yield of 34 ± 0.5% chito-protein. The FTIR spectra of MCSNC.

MCSNC+AE (plus abattoir effluent) and MCSNC+FPE (plus fish pond effluent) are depicted in Fig. 1, the FTIR spectra of MCSNC vibrational peaks observed from the analysis were made at 3324.8, 2922.2, 1570, 1513.3, 1363.5, 1028, 898.3, and 662.4 cm^{-1}. Usually, the absorption peaks observed below 500 cm-1 are not applicable for the characterization of crab shell [10,13]. The strong peaks at 1028 and 662.4 cm-1 may be attributed to Fe-O lattice bending vibration resulting from the fero-magnetic co-precipitation step of MCSNC synthesis. The absorption peak at 898.3 cm^{-1} indicates the existence of aliphatic C-N stretching group in the crab shell. The wave-number at 1363.5 cm^{-1} can be assigned to C-H bending of side chain –CH2OH and presence of β-esters. The absorption peak at 3324.8 cm^{-1} which is within the range of 3300 and 3500 cm^{-1} is characteristic of N-H of amides, [29]. Studies in literature about FTIR spectroscopy related with

crabshell chito-protein showed that characteristic peaks at 2922 cm^{-1}, 1513.3 cm^{-1} and 1570 cm^{-1} are after adsorptive-coagulation treatment of abattoir and fishpond effluents, FTIR results of spent MCSNC (MCSNC+AE and MCSNC+FPE) showed discernible vibrational deviations, and disappearance of some peaks. The N–H bending vibration of amide II band, observed at 1513.3 cm^{-1} in the original adsorbent, completely disappeared following abattoir effluent treatment (MCSNC+AE). Similarly, C-N stretching vibration completely collapsed following treatment of both effluents. These significant reductions and disappearance of peaks illustrate the presence of –CH3, –CH2, N–H bending vibration of amide II band, and N–H bending vibration of primary amides (Choi *et al.*, 2007) and the participation of these functional groups in the treatment of abattoir and fishpond effluents.

4.2 Results of the Experimental Design, RSM, ANOVA and Optimization

The results of experimental design for abattoir waste water coagulation using MCSNC were shown in Table 4.

Table 3. Physicochemical characterization

Parameters	Raw waste water effluent	Treated waste water effluent
Turbidity (mg/L)	595	63
Total suspended solids (mg/L)	1030.8	2.5
Total solids (mg/L)	1614.8	2.1
Biological oxygen demand (mg/L)5	220	8.6
Chemical oxygen demand (mg/L)	692	152
COD/BOD5	3.145	17.67
pH	7.5	8.1
Total phosphorus, mg/L	77.6	4.3
Alkalinity as CaCO3 (mg/L)	1.4217	0.2294
Sulphate as SO4 (mg/L)	13.62	-
Iron (mg/L)	3.08	-
Sodium as Na (mg/L)	35.855	25.1072
Potassium as K (mg/L)	0.5096	0.3579
Oil and grease (mg/L)	1.546	1.1026
Odour	Offensive	Odourless
Colour	Dark red	colourless

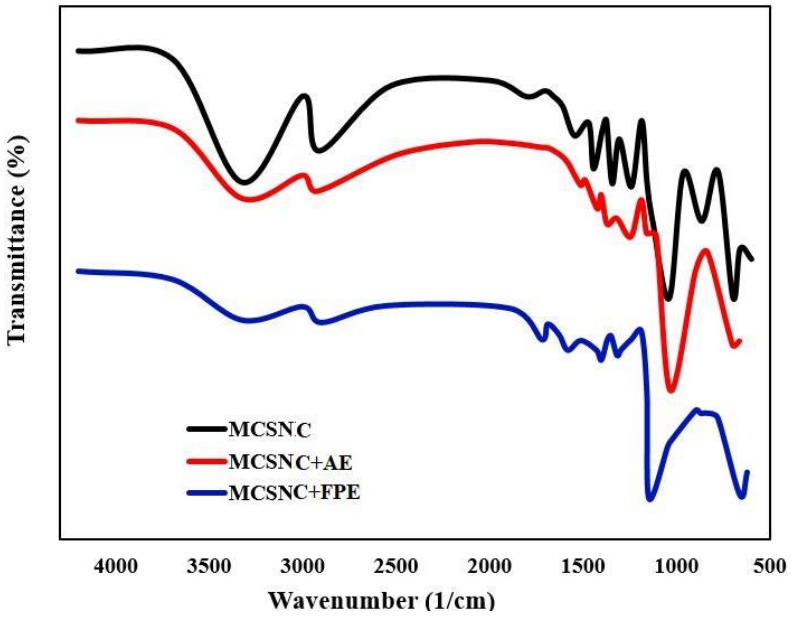

Fig. 1. FTIR spectra of pure and spent nanoparticle (MCSNC)

Table 4. Experimental design with laboratory outcome

Run	pH	dosage	Initial onc (mg/L)	Temp (K)	Time (min)	BOD (mg/L)	COD (mg/L)	Turbidity (%)	Color (%)
1	8	0.50	100.50	310.00	50.00	18.31	180.55	36.09	33.11
2	4	0.50	100.50	310.00	15.00	0.36	176.80	97.74	94.76
3	8	1.10	100.50	310.00	15.00	13.22	193.64	41.33	38.35
4	4	1.10	100.50	310.00	50.00	0.26	155.26	91.61	88.63
5	8	0.50	400.50	310.00	15.00	25.80	212.54	51.44	48.46
6	4	0.50	400.50	310.00	50.00	4.50	174.15	85.42	82.43
7	8	1.10	400.50	310.00	50.00	3.87	168.03	81.17	78.18
8	4	1.10	400.50	310.00	15.00	1.31	184.28	83.38	80.40
9	8	0.50	100.50	345.00	15.00	1.19	196.00	95.42	92.44
10	4	0.50	100.50	345.00	50.00	4.09	157.61	86.16	83.18
11	8	1.10	100.50	345.00	50.00	3.13	153.71	79.15	74.57
12	4	1.10	100.50	345.00	15.00	2.92	149.97	81.27	76.68
13	8	0.50	400.50	345.00	50.00	1.08	150.02	73.65	69.06
14	4	0.50	400.50	345.00	15.00	3.17	136.27	88.06	83.48
15	8	1.10	400.50	345.00	15.00	18.98	180.89	28.90	24.31
16	4	1.10	400.50	345.00	50.00	3.08	142.51	79.09	74.49
17	8	0.50	100.50	327.50	32.50	15.61	153.29	42.54	37.96
18	4	0.50	100.50	327.50	32.50	2.12	123.56	81.83	77.25
19	8	1.10	100.50	327.50	32.50	3.59	164.18	76.17	71.59
20	4	1.10	100.50	327.50	32.50	1.22	153.75	67.90	63.32
21	8	0.50	400.50	327.50	32.50	0.94	162.45	86.92	71.34
22	4	0.50	400.50	327.50	32.50	8.06	159.67	79.10	63.52
23	8	1.10	400.50	301.25	32.50	5.90	157.68	78.56	74.97
24	4	1.10	400.50	353.75	32.50	0.29	124.26	87.46	83.88
25	8	0.50	100.50	327.50	6.25	5.60	140.86	88.82	85.23
26	4	0.50	100.50	327.50	58.75	0.14	113.00	97.96	94.38
27	8	1.10	100.50	327.50	32.50	2.41	125.43	83.01	79.43
28	4	1.10	100.50	327.50	32.50	1.93	104.93	87.26	83.68
29	8	0.50	400.50	327.50	32.50	5.10	128.10	75.32	71.74
30	4	0.50	400.50	327.50	32.50	0.90	116.90	91.08	87.50
31	8	1.10	400.50	327.50	32.50	0.70	123.70	82.59	79.01
32	4	1.10	400.50	327.50	32.50	1.13	124.13	90.23	86.65

The ANOVA table values for BOD linear and interaction models were shown in Table 5 and Table 6 respectively.

The outcome of the ANOVA table for BOD suggests that Interaction model had a higher prediction accuracy when the R-square values were compared.

The comparative analysis between the linear and interaction model predicted outcome was shown in Fig. 2.

From Fig. 2, it was seen that generally, the interaction RSM model predicted BOD had a better prediction than the linear model. This was affirmed by number of coincide points shown in Fig. 2 and affirmed by the statistical analysis performed.

The ANOVA table values for COD linear and interaction models were shown in Table 7 and Table 8 respectively.

The outcome of the ANOVA table for COD suggests that Interaction model had a higher prediction accuracy when the R-square values were compared.

The comparative analysis between the linear model predicted COD and the interaction model predicted COD was shown in Fig. 3.

The outcome in Fig. 3 affirms that the interaction model predicted COD had a better prediction outcome than the linear model predicted COD in terms of tracking of the actual data. This was further affirmed by the statistical analysis performed.

Table 5. ANOVA table for linear model

Coefficient variable	Coefficient values	Sum of square (SE)	T-statistics	P-value	Statistical parameters
a_0	30.4760	25.1811	1.2103	0.2371	R^2 = 0.2989
a_1	1.2683	0.5212	2.4336	0.0221	adjR^2 = 0.1641
a_2	-3.4406	3.4264	-1.0042	0.3246	mse = 33.8112
a_3	0.0018	0.0069	0.2648	0.7933	rmse = 5.8147
a_4	-0.0858	0.0739	-1.1615	0.2560	
a_5	-0.0814	0.0739	-1.1018	0.2807	

Table 6. ANOVA table for Interaction model

Coefficient variable	Coefficient values	Sum of square (SE)	T-statistics	P-value	Statistical parameters
a_0	45.0690	110.9462	0.4062	0.6900	R^2 = 0.6575
a_1	22.9104	11.1817	2.0489	0.0572	adjR^2 = 0.3365
a_2	-159.9352	77.2337	-2.0708	0.0549	mse = 26.8385
a_3	-0.0034	0.1550	-0.0220	0.9827	rmse = 5.1806
a_4	-0.2170	0.3332	-0.6512	0.5241	
a_5	0.6301	1.4133	0.4458	0.6617	
a_6	-0.6824	1.5749	-0.4333	0.6706	
a_7	-0.0013	0.0031	-0.4155	0.6833	
a_8	-0.0586	0.0336	-1.7415	0.1008	
a_9	-0.0410	0.0336	-1.2190	0.2405	
a_{10}	-0.0042	0.0206	-0.2019	0.8425	
a_{11}	0.5158	0.2294	2.2484	0.0390	
a_{12}	-0.2299	0.2294	-1.0023	0.3311	
a_{13}	0.0001	0.0005	0.3158	0.7563	
a_{14}	-0.0010	0.0005	-2.1067	0.0513	
a_{15}	-0.0002	0.0042	-0.0545	0.9572	

Table 7. Linear model

Coefficient variable	Coefficient values	Sum of square (SE)	T-statistics	P-value	Statistical parameters
a_0	339.6797	105.4300	3.2219	0.0034	R^2 = 0.2879
a_1	3.7392	2.1820	1.7136	0.0985	adjR^2 = 0.1510
a_2	-7.8563	14.3458	-0.5476	0.5886	mse = 592.7065
a_3	0.0006	0.0287	0.0221	0.9826	rmse = 24.3456
a_4	-0.5741	0.3094	-1.8555	0.0749	
a_5	-0.4680	0.3094	-1.5126	0.1424	

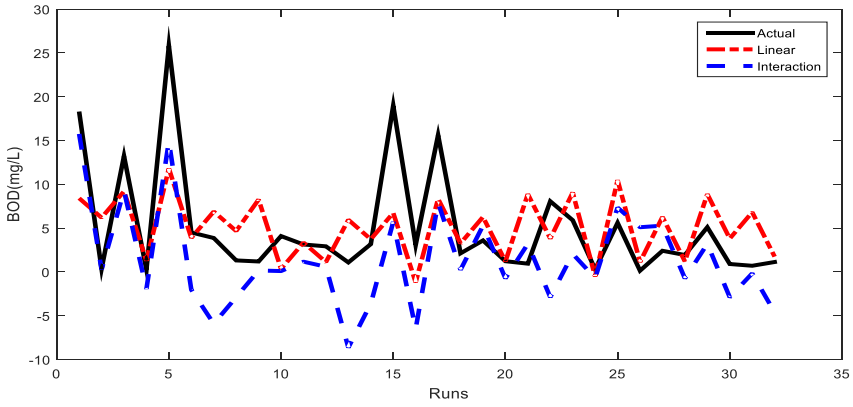

Fig. 2. BOD RSM prediction comparative plot

Table 8. Interaction model

Coefficient variable	Coefficient values	Sum of square (SE)	T-statistics	P-value	Statistical parameters
a_0	532.6513	641.5447	0.8303	0.4186	R^2 = 0.3365
a_1	-18.9370	64.6581	-0.2929	0.7734	adjR^2 = 0.0117
a_2	-141.9645	446.6027	-0.3179	0.7547	mse = 897.4009
a_3	0.5839	0.8963	0.6514	0.5240	rmse = 29.9567
a_4	-1.3246	1.9269	-0.6874	0.5017	
a_5	-1.6891	8.1727	-0.2067	0.8389	
a_6	-3.1302	9.1067	-0.3437	0.7355	
a_7	-0.0077	0.0182	-0.4230	0.6779	
a_8	0.0872	0.1944	0.4485	0.6598	
a_9	-0.0415	0.1944	-0.2134	0.8337	
a_{10}	0.0076	0.1194	0.0639	0.9499	
a_{11}	0.5163	1.3264	0.3893	0.7022	
a_{12}	-0.5143	1.3264	-0.3877	0.7033	
a_{13}	-0.0016	0.0027	-0.6012	0.5561	
a_{14}	-0.0006	0.0027	-0.2082	0.8377	
a_{15}	0.0061	0.0245	0.2503	0.8056	

Table 9. Linear model

Coefficient variable	Coefficient values	Sum of square (SE)	T-statistics	P-value	Statistical parameters
a_0	72.7069	73.0403	0.9954	0.3287	R^2=0.2530
a_1	-4.1383	1.5117	-2.7376	0.0110	adjR^2=0.1093
a_2	-4.0073	9.9385	-0.4032	0.6901	mse=284.4702
a_3	0.0017	0.0199	0.0850	0.9329	rmse=5.8147
a_4	0.0893	0.2144	0.4166	0.6804	
a_5	0.0939	0.2144	0.4380	0.6650	

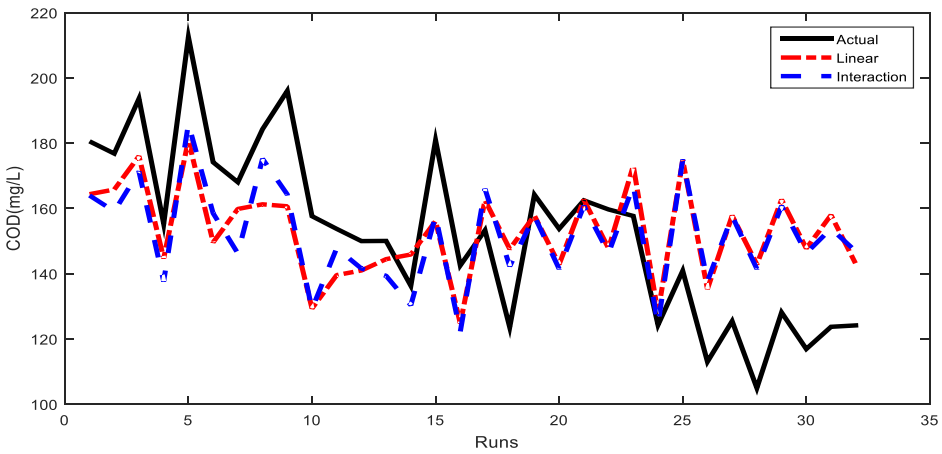

Fig. 3. COD RSM prediction comparative plot

The ANOVA table values for turbidity linear and interaction models were shown in Table 9 and Table 10 respectively.

The outcome of the ANOVA table for Turbidity suggests that Interaction model had a higher prediction accuracy when the R-square values were compared.

The comparative plots of the linear and interaction models to the actual data were shown in Fig. 4.

Table 10. Interaction model

Coefficient variable	Coefficient values	Sum of square (SE)	T-statistics	P-value	Statistical parameters
a_0	-104.2513	333.8372	-0.3123	0.7589	R^2 = 0.6073
a_1	-42.7905	33.6458	-1.2718	0.2216	adjR^2 = 0.2392
a_2	247.4808	232.3963	1.0649	0.3027	mse = 242.9947
a_3	0.5972	0.4664	1.2805	0.2186	rmse = 15.5883
a_4	0.8685	1.0027	0.8662	0.3992	
a_5	-1.8755	4.2528	-0.4410	0.6651	
a_6	2.4493	4.7388	0.5169	0.6123	
a_7	0.0032	0.0095	0.3421	0.7367	
a_8	0.1045	0.1012	1.0333	0.3168	
a_9	0.0235	0.1012	0.2322	0.8194	
a_{10}	0.0088	0.0621	0.1419	0.8889	
a_{11}	-0.9715	0.6902	-1.4074	0.1784	
a_{12}	1.5584	0.6902	2.2577	0.0383	
a_{13}	-0.0021	0.0014	-1.4982	0.1536	
a_{14}	0.0018	0.0014	1.2715	0.2217	
a_{15}	0.0008	0.0127	0.0642	0.9496	

Table 11. Linear model

Coefficient variable	Coefficient values	Sum of square (SE)	T-statistics	P-value	Statistical parameters
a_0	76.7845	73.9548	1.0383	0.3087	R^2=0.2441
a_1	-4.1611	1.5306	-2.7186	0.0115	adjR^2=0.0987
a_2	-1.8438	10.0630	-0.1832	0.8560	mse=291.6379
a_3	-0.0032	0.0201	-0.1567	0.8767	rmse=17.0774
a_4	0.0621	0.2170	0.2862	0.7770	
a_5	0.0935	0.2170	0.4306	0.6703	

Table 12. Interaction model

Coefficient variable	Coefficient values	Sum of square (SE)	T-statistics	P-value	Statistical parameters
a_0	-104.2513	333.8372	-0.3123	0.7589	R^2=0.5974
a_1	-42.7905	33.6458	-1.2718	0.2216	adjR^2=0.2200
a_2	247.4808	232.3963	1.0649	0.3027	mse=252.4036
a_3	0.5972	0.4664	1.2805	0.2186	rmse=15.8872
a_4	0.8685	1.0027	0.8662	0.3992	
a_5	-1.8755	4.2528	-0.4410	0.6651	
a_6	2.4493	4.7388	0.5169	0.6123	
a_7	0.0032	0.0095	0.3421	0.7367	
a_8	0.1045	0.1012	1.0333	0.3168	
a_9	0.0235	0.1012	0.2322	0.8194	
a_{10}	0.0088	0.0621	0.1419	0.8889	
a_{11}	-0.9715	0.6902	-1.4074	0.1784	
a_{12}	1.5584	0.6902	2.2577	0.0383	
a_{13}	-0.0021	0.0014	-1.4982	0.1536	
a_{14}	0.0018	0.0014	1.2715	0.2217	
a_{15}	0.0008	0.0127	0.0642	0.9496	

The comparative plot in Fig. 4 affirms that interaction model had a better outcome as it had a better closeness to the actual data than that of the linear model predicted data. Hence, interaction model presents a better optimal position than the linear model.

The ANOVA table values for colour response of linear and interaction models was shown in Table 11 and Table 12 respectively.

The outcome of the ANOVA table for Turbidity suggests that Interaction model had a better

prediction accuracy when the R-square values were compared

The comparative plots of the linear and interaction model were shown in Fig. 5.

Fig. 5 affirms that the interaction model had a better prediction than the linear model and the prediction tracking deviation was lower in the interaction model data prediction than the linear model.

From the ANOVA table and the comparative plots presented, it was seen that interaction model had the best prediction accuracy and was used for the genetic algorithm optimization with the optimization iterations shown in Table 13.

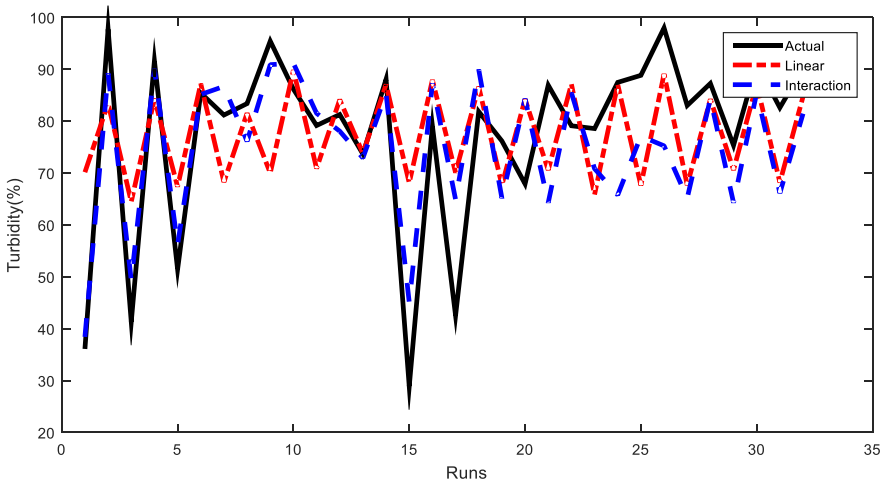

Fig. 4. Turbidity RSM prediction comparative plot

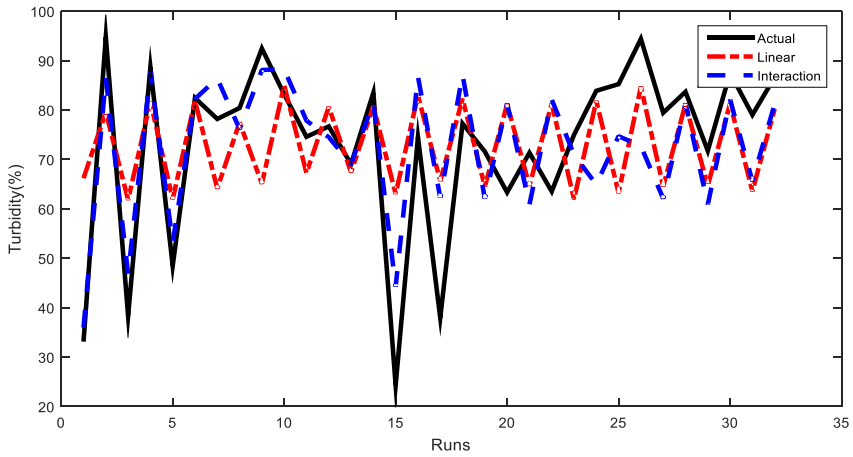

Fig. 5. Colour RSM prediction comparative plot

Table 13. Optimum conditions obtained with genetic algorithm

Responses and factors	Optimal conditions
BOD(mg/L)	4.33
COD(mg/L)	128.9
Turbidity (%)	39.87
Colour (%)	33.41
pH	5.5
Dosage(g)	0.68
Initial Concentration (mg/L)	260
Temperature (K)	335
Time (min)	50

The optimal response and the optimal conditions required to achieve the optimal repose executed in genetic algorithm was presented in Table 13. At temperature of 335K, Initial concentration of 260mg/L, time of 50mins and dosage of 0.68g, the optimal responses of BOD 4.33mg/L, COD of 128.9mg/L, turbidity of 39.87% and colour of 33.41% were achieved.

5. CONCLUSION

This paper presented the purification process of Abattoir waste water using the synthesized nanoparticles of crab shells. The experimental design was carried out with central composite design (CCD) based on pH, dosage, initial concentration, temperature and time factors and the number of levels and number of experimental runs obtained were 5 and 50 respectively. The responses considered were BOD, COD, turbidity and color. The outcome of the design was taken to the laboratory to generate the values of the responses. The outcome of the experiment was subjected to the linear and interaction RSM models with ANOVA used to determine the performance of the models. It was found that interaction model had the best prediction performance and the outcome of the model was subjected genetic algorithm optimization. From the results obtained, it was found that at temperature of 335K, Initial concentration of 260mg/L, time of 50mins and dosage of 0.68g, the optimal responses of BOD 4.33mg/L, COD of 128.9mg/L, turbidity of 39.87% and colour of 33.41% were achieved.

For the suggestions for further studies, artificial intelligence models should be utilized in the prediction of the responses and should be compared with the outcome of the RSM models. Crab shell synthesized nanoparticles should be utilized in the purification of other waste waters.

COMPETING INTERESTS

Authors have declared that no competing interests exist.

REFERENCES

1. Aniagor CO, Menkiti MC. Kinetics and mechanistic description of adsorptiveuptake of crystal violet dye by lignifed elephant grass complexed isolate. J EnvironChem Eng; 2018.
Available:https://doi.org/10.1016/j.jece.2018.01.070
2. Ali A, Zafar H, Zia M, Haq I, Phull AR, Ali JS, Hussain A. Synthesis, characterization, applications, and challenges of iron oxide nanoparticles, Nanotechnology, Science and Applications; 2016.
Available:http://dx.doi.org/10.2147/NSA.S99986
3. Adeogun O, Solarin B. Ambrose E. Ogunbadejo H, Bolaji D, Orimogunje R, Ajulo , Olusola A, Aroriode R, Adeogun M. Crab fishing and socio-economic considerations in lagos lagoon system in Nigeria. Int. J. Fish. Aquacult. 2011;3:118–125.
4. Braul L, Viraraghavan V, Corkal D. Cold water effects on enhanced coagulation of high DOC, low turbidity water, water qual. Res. J. Canada. 2001; 36(4): 701–717
5. Birima AH, Hammad HA, et al. Extraction of natural coagulant from peanut seeds for treatment of turbid water. IOP Conf Series Earth Environ Sci. 2013;16:1–4.
6. Elemile OO, Raphael DO, Omole DO, Oloruntoba EO, Ajayi EO, Ohwavborua NA. Assessment of the impact of abattoir efuent on the quality of groundwater in a residential area of Omu-Aran, Nigeria. Environ Sci Eur. 2019;31:16.
Available:https://doi.org/10.1186/s12302-019-0201-5
7. Ejımofor MI, Menkiti MC, Ezemagu IG. Comparative studies on removal of turbid-metric particles (TDSP) using animal based chito-protein and aluminium sulfate on paint wastewater (PWW). Sigma Journal of Engineering and Natural Sciences. 2020a;38(3):1143-1159.
8. Ejimofor MI, Ezemagu G, Menkiti MC. Biogas production using coagulation sludge obtained from paint wastewater decontamination: Characterization and anaerobic digestion kinetics, Current Research in Green and Sustainable Chemistry. 2020b;3:100024.
Available:https://doi.org/10.1016/j.crgsc.2020.100024.
9. Hatamie A, Parham H, Zargar B, Heidari Z. Evaluating magnetic nano-ferrofluid as a novel coagulant for surface water treatment. Journal of Molecular Liquids. 2016;219:694–702.
Available:http://dx.doi.org/10.1016/j.molliq.2016.04.020
10. Jeon C. Removal of Cr (VI) from aqueous solution using amineimpregnated crab

shells in the batch process. J Ind Eng Chem. 2019;77:111–117.
11. Kundu P, Debsarkar A, Mukherjee S. Treatment of slaughter house waste water in a sequencing batch reactor: Performance evaluation and biodegradation kinetics, BioMed Res. Int. 2013;11:1–15.
12. Kristianto H, Reynaldi E, Prasetyo S, Sugih A. Adsorbed leucaenaprotein on citrate modified Fe3O4 nanoparticles: synthesis, characterization, and its application as magnetic coagulant. Sustainable Environment Research. 2020;30:32 Available:https://doi.org/10.1186/s42834-020-00074-4.
13. Okey-Onyesolu CF, Chukwuma EC, Okoye CC, Onukwuli OD. Response surface methodology optimization of chito-protein synthesized from crab shell in treatment of abattoir wastewater. Heliyon. 2020;6(10):e05186. Available:https://doi.org/10.1016/j.heliyon.2020.e04468
14. Okuda T, Baes AU, et al. Improvement of extraction method of coagulation active components from moringa oleifera seed. Wat Res. 1993;33(15):3373–3378.
15. Okey-Onyesolu CF, Chukwuma EC, Okoye CC, Onukwuli OD. Response surface methodology optimization of chito-protein synthesized from crab shell in treatment of abattoir wastewater. Heliyon. 2020b;e04468. Available:https://doi.org/10.1016/j.heliyon.2020.e04468
16. Ogbeide OA. Meat industry development in nigeria: implications of the consumers' perspective. Mayfair J Agribus Manag. 2015;1:59–75.
17. Ohale PE, Onu CE, Nwabanne JT, Aniagor CO, Okey-Onyesolu CF, Ohale NJ. A comparative optimization and modeling of ammonia–nitrogen adsorption from abattoir wastewater using a novel iron-functionalized crab shell. Applied Water Science. 2022;12:193. Available:https://doi.org/10.1007/s13201-022-01713-4
18. Ohale PE, Onu CE, Ohale NJ, Oba SN. Adsorptive kinetics, isotherm and thermodynamic analysis of fishpond effluent coagulation using chitin derived coagulant from waste Brachyura shell. Chemical Engineering Journal Advances. 2020;4:100036. Available:https://doi.org/10.1016/j.ceja.2020.100036
19. Onu CE, Nwabanne JT, Ohale PE, Asadu CO. Comparative analysis of RSM, ANN and ANFIS and the mechanistic modeling in eriochrome black-T dye adsorption using modified clay, South African Journal of Chemical Engineering 2021;36:24 – 42. Available:https://doi.org/10.1016/j.sajce.2020.12.003
20. Panagopoulos A. Energetic, economic and environmental assessment of zero liquid discharge (ZLD) brackish water and seawater desalination systems. Energy Conversion and Management. 2021;235.
21. Panagopoulos A. Study and evaluation of the characteristics of saline wastewater (brine) produced by desalination and industrial plants. Environ Sci Pollut Res. 2022;29:23736–23749. Available:https://doi.org/10.1007/s11356-021-17694-x
22. Santos TRTd, Silva MF, et al. Magnetic coagulant based on moringa oleifera seeds extract and super paramagnetic nanoparticles: optimization of operational conditions and reuse evaluation. Desalin Water Treat. 2018;106:226–237.
23. Santos TRTd, Mateus GAP, et al. A simple and effective method for escherichia coli inactivation in aqueous medium using natural based superparamagnetic coagulant. Environ Prog Sustain Energy. 2021;40(2):e13503.
24. Soenen SJ, Himmelreich U, Nuytten N, Pisanic TR 2nd, Ferrari A, De Cuyper M. Intracellular nanoparticle coating stability determines nanoparticle diagnostics efficacy and cell functionality. Small. 2010;6(19):2136–2145
25. Tan K, Hameed B. Insight into the adsorption kinetics models for the removal of contaminants from aqueous solutions. J. Taiwan Inst. Chem. Eng. 2017;74:25–48.
26. Von Sperling M, Chernicharo CA. Urban wastewater treatment technologies and the implementation of discharge standards in developing countries. Urban Water. 2002;1:105–114.
27. Wang N, Xu Z, Xu W, Xu J, Chen Y, Zhang M. Comparison of coagulation and magnetic chitosan nanoparticle adsorption on the removals of organic compound and coexisting humic acid: A case study with salicylic acid. Chemical Engineering Journal. 2018;347:514–524.

Available:https://doi.org/10.1016/j.cej.2018.04.131

28. Wang Y, Gu X, Quan J, et al. Application of magnetic fields to wastewater treatment and its mechanisms: A review. Science of the Total Environment. 2021;773:145476. Available:https://doi.org/10.1016/j.scitotenv.2021.145476

29. Okuda T, Baes AU, et al. Improvement of extraction method of coagulation active components from moringa oleifera seed. Wat Res. 1999;33(15):3373–3378.

Peer-review history:
The peer review history for this paper can be accessed here:
https://www.sdiarticle5.com/review-history/112128